

Effect of back diffusion on overall solidification kinetics of undercooled single-phase solid-solution alloys

WANG Hai-feng, LIU Feng, WANG Kang, ZHAI Hai-min

State Key Laboratory of Solidification Processing, Northwestern Polytechnical University, Xi'an 710072, China

Received 9 September 2011; accepted 4 January 2012

Abstract: Departing from the volume-averaging method, an overall solidification kinetic model for undercooled single-phase solid-solution alloys was developed to study the effect of back diffusion on the solidification kinetics. Application to rapid solidification of undercooled Ni–15%Cu (mole fraction) alloy shows that back diffusion effect has significant influence on the solidification ending temperature but possesses almost no effect on the volume fraction solidified during recalcence. Inconsistent with the widely accepted viewpoint of Herlach, solidification ends at a temperature between the predictions of Lever rule and Scheil's equation, and the exact value is determined by the effect of back diffusion, the initial undercooling and the cooling rate.

Key words: Ni–Cu alloy; rapid solidification; diffusion; undercooling

1 Introduction

The major aim of solidification science is to optimize the mechanical and physical properties of solidified alloys by microstructure control. Such an aim can be fulfilled, which provides that the whole solidification process, including liquid-cooling, solidification and solid-cooling, is fully understood. Therefore, modeling the overall solidification kinetics, where the macroscopic and microscopic models are coupled (i.e. micro-macroscopic approach [1]), becomes quite important, since it gives a more accurate assessment of the quality and ultimately gives the mechanical properties of the solidified product.

An original model was proposed by RAPPAPAZ and THÉVOZ (RT) [2] for equiaxed dendritic growth under near-equilibrium conditions. Using the volume-averaging method [3], a more general model was subsequently developed by WANG and BECKERMAN (WB) [4]. Since then, many improved works have been carried out [5–7], but limit themselves to near-equilibrium solidification. With the development of non-equilibrium solidification technologies, rapid solidification of

undercooled melts has become a hot-spot in solidification science. However, as a successful method to produce novel metastable phases and microstructures [8–10], it did not cause sufficient concern in modeling the overall solidification kinetics. As the first step, an overall solidification kinetic model without considering the effect of back diffusion was proposed for rapid solidification of undercooled single-phase solid-solution alloys [11,12].

Back diffusion is not critical for a good agreement between the predicted and measured cooling curves, but is very important in the overall solidification kinetics (e.g. it influences the solidification ending temperature [11,12]) and should be taken into consideration. In the present work, back diffusion is further incorporated in the model of WANG et al [11] and its effect on the overall solidification kinetics is studied in detail, based on the model calculation results in undercooled Ni–15%Cu (mole fraction) alloy.

2 Model derivation

Following the RT [2] and WB [4] models, the grain envelope is defined as a fictitious spherical surface

Foundation item: Project (2011CB610403) supported by the National Basic Research Program of China; Project (51125002) supported by the National Science Fund for Distinguished Young Scholars of China; Projects (51101122, 51071127, 50901059) supported by the National Natural Science Foundation of China; Project (111502) supported by the Huo Yingdong Young Teacher Fund, China; Projects (66-QP-2010, 24-TZ-2009) supported by the Free Research Fund of State Key Laboratory of Solidification Processing, China; Projects (JC201008, JC200801) supported by the Fundamental Research Fund of Northwestern Polytechnical University, China; Project (B08040) supported by the Program of Introducing Talents of Discipline to Universities, China

Corresponding author: LIU Feng; Tel: +86-29-88460374; E-mail: liufeng@nwpu.edu.cn

DOI: 10.1016/S1003-6326(11)61226-0

stretched by (or around) the dendrite tip, and the spherical grain for dendritic growth is divided into three different regions or phases, i.e. the solid dendrite s , the inter-dendritic liquid l_i , and the extra-dendritic liquid l_e , where s and l_e are only in pointwise contact and the corresponding interfacial area is ignored. If the densities of s , l_i and l_e are equal and constant, the solute diffusion in the macroscopic scale is omitted, and the solute diffusion in l_i and l_e is under quasi-steady states and back diffusion in s is considered, the solute balances for s , l_i and l_e , respectively, can be, according to the volume-averaging method [3] obtained as:

$$g^s \frac{\partial \langle C^s \rangle^s}{\partial t} = \left(kC_1^* - \langle C^s \rangle^s \right) \left(\frac{\partial g^s}{\partial t} + S^s \frac{D^s}{l_C^{sl_i}} \right) \quad (1)$$

$$g^{l_i} \frac{\partial \langle C^{l_i} \rangle^{l_i}}{\partial t} = \left(\langle C^{l_i} \rangle^{l_i} - kC_1^* \right) \frac{\partial g^s}{\partial t} - \left(C^e - \langle C^{l_i} \rangle^{l_i} \right) \frac{\partial g^{l_e}}{\partial t} - S^s \frac{D^s}{l_C^{sl_i}} \left(kC_1^* - \langle C^s \rangle^s \right) - \left(C^e - \langle C^{l_e} \rangle^{l_e} \right) S^e \frac{D^{l_e}}{l_C^{l_i l_e}} \quad (2)$$

$$g^{l_e} \frac{\partial \langle C^{l_e} \rangle^{l_e}}{\partial t} = \left(C^e - \langle C^{l_e} \rangle^{l_e} \right) \left(S^e \frac{D^{l_e}}{l_C^{l_i l_e}} + \frac{\partial g^{l_e}}{\partial t} \right) \quad (3)$$

where $\langle \rangle$ is an averaging operator [3]; $g^s(\langle C^s \rangle^s)$, $g^{l_i}(\langle C^{l_i} \rangle^{l_i})$ and $g^{l_e}(\langle C^{l_e} \rangle^{l_e})$ are respectively the volume fractions (the averaged concentration) of s , l_i and l_e ; C_1^* and C^e are the averaged concentrations of liquid at the s - l_i and l_i - l_e interfaces; k is the non-equilibrium partition coefficient; $l_C^{sl_i}$ and $l_C^{l_i l_e}$ are respectively the solute diffusion length in s and l_e at the s - l_i and l_i - l_e interfaces; S^s and S^e are the interfacial area concentrations for the s - l_i and l_i - l_e interfaces; D^s and D^{l_e} are respectively the solute diffusion coefficients of the solid (s) and the liquid (l_i and l_e), and

$$\psi^{l_e} = \begin{cases} 1 - v^2 / v_D^2, & v < v_D \\ 0, & v \geq v_D \end{cases} \quad (4)$$

where v is the growth velocity of the grain envelope (i.e., the l_i - l_e interface) and v_D is the velocity of solute diffusion in the liquid (l_i and l_e), which are introduced to account for the effect of non-equilibrium solute diffusion [13,14]. Note that Eqs. (1)–(3) are the same as that in Ref. [11], except that a term $\left(kC_1^* - \langle C^s \rangle^s \right) S^s D^s / l_C^{sl_i}$

is introduced in Eqs. (1) and (2) to account for the effect of back diffusion.

If the latent heat of solidification is constant (ΔH_f), the specific heat capacities of s , l_i and l_e are equal and constant (c_p), heat diffusion in the macroscopic scale is

omitted, heat diffusion in l_e is under a quasi-steady state, heat diffusion of s and l_i is not considered, and the temperatures of s and l_i are equal (T_i), the energy balance for the mushy zone (s and l_i) and the extra-dendritic liquid (l_e), respectively, can be, according to the volume-averaging method [3] obtained as:

$$\frac{\partial g^s}{\partial t} = \left[(1 - g^{l_e}) \frac{\partial T_i}{\partial t} + S^e \frac{\alpha^l}{l_T^{l_i l_e}} \left(T_i - \langle T^{l_e} \rangle^{l_e} \right) \right] / \frac{\Delta H_f}{c_p} \quad (5)$$

$$g^{l_e} \frac{\partial \langle T^{l_e} \rangle^{l_e}}{\partial t} = \left(S^e \frac{\alpha^l}{l_T^{l_i l_e}} + \frac{\partial g^{l_e}}{\partial t} \right) \left(T_i - \langle T^{l_e} \rangle^{l_e} \right) - \phi \quad (6)$$

where $\langle T^{l_e} \rangle^{l_e}$ is the averaged temperature of l_e ; $l_T^{l_i l_e}$ is the heat diffusion length in l_e at the l_i - l_e interface; α^l is the thermal diffusivity; ϕ is the cooling rate.

Depending on the growth kinetics of the s - l_i interface, dendritic grain growth can be classified into three stages, i.e., 1) purely thermal-controlled growth, 2) mainly thermal-controlled growth and 3) solute-diffusion controlled growth [11]. Since the growth kinetics of the s - l_i interface can be described by either the solute or the energy balance, e.g., for stages (1) and (2), the energy balance of the mushy zone (i.e. Eq. (5)) is applied; whereas for stage (3), the solute balance at the s - l_i interface, i.e.,

$$\frac{\partial g^s}{\partial t} = S^s \left[\frac{D^s}{l_C^{sl_i}} \left(kC_1^* - \langle C^s \rangle^s \right) + \frac{D^{l_i}}{l_i} \left(C_1^* - \langle C^{l_i} \rangle^{l_i} \right) \right] / C_1^* (1 - k) \quad (7)$$

is adopted. The transition from thermal-controlled to solute-diffusion controlled growth is assumed to happen once the growth rate predicted by Eq. (7) is larger than that by Eq. (5). As to the growth kinetics of the grain envelope, an extended dendrite growth model developed recently [15,16] is applied to obtaining v , T_i , C_1^* and k , which is similar to the treatment in the RT [2] and WB [4] models.

For globular grain growth, there is no l_i any more and the grain envelope coincides with the s - l_e interface, i.e., $g^s = 1 - g^{l_e}$ and $S^s = S^e$. In this case, the solute balance for s follows Eq. (1) and the solute balance for l_e according to the volume-averaging method [3] can be obtained as:

$$g^{l_e} \frac{\partial \langle C^{l_e} \rangle^{l_e}}{\partial t} = \left(kC_1^* - \langle C^{l_e} \rangle^{l_e} \right) \frac{\partial g^{l_e}}{\partial t} - \left(kC_1^* - \langle C^s \rangle^s \right) S^s \frac{D^s}{l_C^{sl_e}} \quad (8)$$

As to the growth kinetics of the s–l_e interface, it can be obtained from the solute balance as

$$\frac{\partial g^s}{\partial t} = S^s \left[\frac{D^s}{l_c^{sl_e}} \left(kC_1^* - \langle C^s \rangle^s \right) + \frac{D^l}{l_c^{ls}} \left(C_1^* - \langle C^{l_e} \rangle^{l_e} \right) \right] / C_1^* (1-k) \quad (9)$$

where $l_c^{sl_e}$ and l_c^{ls} are respectively the solute diffusion length in s and l_e at the s–l_e interface.

Generally, globular grain growth happens in two cases [11]. Case 1: at the initial stage of solidification for sufficient small initial undercooling, ΔT , the predicted volume fraction of s (g^s) is larger than that of the mushy zone ($g^s + g^{l_i}$) if the inter-dendritic liquid l_i is presented; Case 2: at the late stage of solidification, the growth of the s–l_i interface is controlled by the external heat extraction, and the growth of the grain envelope slows down due to soft impingement. Thus l_i is consumed gradually until the growth of the remaining l_e starts with $g^{l_i} = 0$, namely, a globular grain growth happens. For both cases (1) and (2), the undercooling is so small that a uniform temperature by Eqs. (5) and (6) reduces to

$$\frac{\partial T}{\partial t} = \frac{\Delta H_f}{c_p} \frac{\partial g^s}{\partial t} - \phi \quad (10)$$

In other words, the globular grain growth is solute-diffusion controlled.

Subjected analogous treatments to nucleation, and thermal and solute diffusion impingements as that in Ref. [11], an extended overall solidification kinetic model incorporating the effect of back diffusion was established for undercooled single-phase solid-solution alloys, where the expressions for the interfacial area concentration, the solute diffusion length and the thermal diffusion length can be found in Ref. [11].

3 Results and discussion

The present model is adopted to describe the overall solidification kinetics of undercooled Ni-15%Cu (mole fraction) alloy. Values of the physical parameters are available in Ref. [12]. From HERLACH [8], the solidification process can be divided into two stages.

1) Recalescence: Once solidification initiates, primary crystallization takes place under non-equilibrium condition and the volume fraction solidified during recalescence g_R can be determined by

$$g_R = \frac{\Delta T}{\Delta H_f / c_p} = \frac{\Delta T}{\Delta H_{hyp}} \quad (11)$$

where ΔH_{hyp} is the hypercooling limit.

2) Post- recalescence: The remaining liquid with a

volume fraction of 1– g_R solidifies under near-equilibrium condition within the melting interval $\Delta T_0 = T_L(C_0) - T_S(C_0)$ with $T_L(C_0)$ and $T_S(C_0)$ respectively as the liquidus and solidus temperature for the initial solute concentration C_0 .

In what follows, the effect of back diffusion on both the recalescence and post-recalescence stages was studied. For a better description, two different values of D_s (i.e. $D_s = 3 \times 10^{-11} \text{ m}^2/\text{s}$, $D_s/D_l = 10^{-2}$ and $D_s = 3 \times 10^{-13} \text{ m}^2/\text{s}$, $D_s/D_l = 10^{-4}$) and ϕ (i.e. $\phi = 50 \text{ K/s}$ and $\phi = 225 \text{ K/s}$) were chosen.

Evolution of g_R with ΔT predicted by the present model and Eq. (12) is shown in Fig. 1. Similar to the model predictions without considering the effect of back diffusion [12], g_R increases linearly with ΔT and the present model predictions almost coincide with that of Eq. (12). This indicates that back diffusion has not enough time to proceed within such a short recalescence stage, and thus it possesses almost no effect on g_R . Note that relatively larger derivations between the present model predictions and that of Eq. (12) occur for low ΔT where the solidification rate is smaller and the near-adiabatic condition is less fulfilled during recalescence (see Fig. 1).

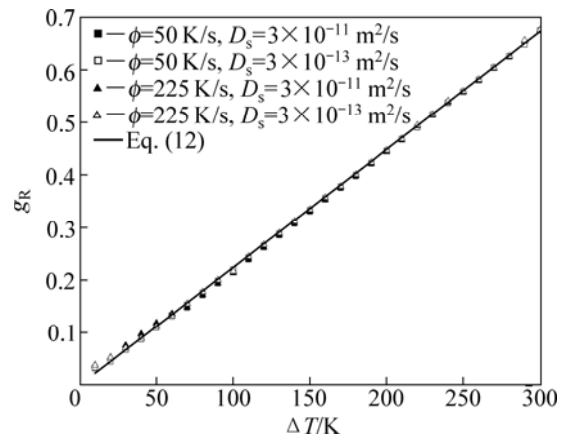


Fig. 1 Volume fraction solidified during recalescence (g_R) as function of initial undercooling (ΔT) predicted by the present model and Eq. (12) for undercooled Ni-15%Cu (mole fraction) alloy

Following the above description of HERLACH [8], after recalescence, solidification should end at $T_S(C_0)$, i.e. $T_{end} = T_S(C_0)$ with T_{end} as the solidification ending temperature. Actually, solidification of undercooled melt is so rapid that solute mixture in the solid and the liquid cannot be performed well, namely, Lever rule is not fulfilled and $T_{end} \neq T_S(C_0)$. Meanwhile, the cooling rate after recalescence is not quick enough to suppress completely the effect of back diffusion, namely, Scheil's equation is not fulfilled and $T_{end} \neq T_m^{Cu}$ (the melting temperature of pure Cu). On this basis, it seems

reasonable and necessary to reexamine T_{end} , particularly incorporating the effect of back diffusion by the present model. Evolution of T_{end} with ΔT is predicted by the present model with different D_s and ϕ (see Fig. 2). Independent of ΔT , T_{end} distributes between $T_s(C_0)$ and T_m . In other words, if back diffusion is considered, solidification then ends at a temperature between the prediction of Lever rule ($T_s(C_0)$) and Scheil's equation (T_m^{Cu}).

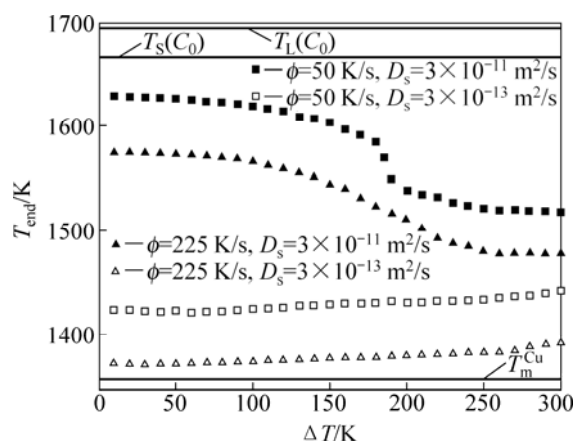


Fig. 2 Solidification ending temperature (T_{end}) as function of initial undercooling (ΔT) predicted by the present model for undercooled Ni–15%Cu (mole fraction) alloy

The exact value of T_{end} is determined by the effect of back diffusion, the initial undercooling and the cooling rate (see Fig. 2). The values of D_s and ϕ determine respectively the effect of back diffusion and the solidification time. Considering the effect of back diffusion, the influence of ΔT on T_{end} should be analyzed from two points of view. On one hand, increasing ΔT equals intensifying the effect of solute trapping, thus reducing the solute gradient in the solid at the solid–liquid interface and weakening the effect of back diffusion (i.e. decreasing T_{end}). This is denoted as Effect (1). On the other hand, increasing ΔT leads to a linear decrease of the volume fraction solidified during post-recalcescence stage (see Fig. 1), thus reducing the release of latent heat that should be extracted to the environment (i.e. increasing T_{end} for a fixed ϕ). This is denoted as Effect (2). For a high value of D_s (e.g. $D_s=3\times 10^{-11} \text{ m}^2/\text{s}$), effect of back diffusion is so strong that Effect 1 and Effect 2 are equally important for T_{end} . As shown by the filled squares and filled triangles in Fig. 2, T_{end} decreases slowly at small ΔT , rapidly at medium ΔT and slowly again at high ΔT . This is due to the completion and transition between Effect (1) and Effect (2), namely, for small ΔT , both Effect (1) and Effect (2) are weak, but with increasing ΔT , Effect (1) becomes dominant at medium ΔT and is replaced by Effect (2) at high ΔT . For a small value of D_s (e.g.

$D_s=3\times 10^{-13} \text{ m}^2/\text{s}$), effect of back diffusion is sufficiently weak and can be neglected, Thus Effect (2) is always dominant and T_{end} increases with ΔT (See the open squares and open triangles in Fig. 2). Furthermore, if ϕ is high (e.g. $\phi=225 \text{ K/s}$), the substantial decrease of solidification time will suppress the effect of back diffusion, so that solidification will end at relatively high temperature (See the solid and open squares and solid and open triangles in Fig. 2).

Such an examination of the overall solidification kinetics is very important in our understanding of the rapid solidification phenomena and the formation of novel metastable phases and microstructures. For example, the above description for the post-recalcescence stage by HERLACH [8] is widely accepted, based on which the plateau duration was measured to predict grain refinement [17,18]. According to the present model, however, solidification generally does not yet complete at the solidus temperature, so that the measured plateau duration in Refs. [17,18] is actually underestimated. On this basis, the grain refinement model of KARMA et al [17,18] should be extended and the present overall solidification kinetic model is very helpful in predicting the plateau duration as well as analyzing the effect of back diffusion on grain refinement [19].

4 Conclusions

1) Due to the short time span of recalcescence, back diffusion possesses almost no effect on the volume fraction solidified in this stage.

2) Incorporating back diffusion, solidification should end at a temperature between the prediction of Lever rule and Scheil's equation, and the exact value is determined by the effect of back diffusion, the initial undercooling and the cooling rate.

References

- [1] RAPPAZ M. Modelling of microstructure of formation in solidification process [J]. International Materials Reviews, 1989, 34: 93–123.
- [2] RAPPAZ M, THÉVOZ P H. Solute diffusion model for equiaxed dendritic growth [J]. Acta Metallurgica, 1987, 35: 1487–1497.
- [3] BECKERMANN C, VISKANTA R. Mathematical modeling of transport phenomena during alloy solidification [J]. Applied Mechanics Reviews, 1993, 46: 1–27.
- [4] WANG C Y, BECKERMANN C. Multiphase solute diffusion model for dendritic alloy solidification [J]. Metallurgical and Materials Transactions A, 1993, 24: 2787–2802.
- [5] RAPPAZ M, BOETTINGER W J. On dendritic solidification of multicomponent alloys with unequal liquid diffusion coefficients [J]. Acta Materialia, 1999, 47: 3205–3219.
- [6] MARTORANO M A, BECKERMANN C, GANDIN CH-A. A solutal interaction mechanism for the columnar-to-equiaxed transition in alloy solidification [J]. Metallurgical and Materials Transactions A, 2003, 34: 1657–1674.

- [7] GANDIN CH-A, MOSBAH S, VOLKMANN T H, HERLACH D M. Experimental and numerical modeling of equiaxed solidification in metallic alloys [J]. *Acta Materialia*, 2008, 56: 3023–3035.
- [8] HERLACH D M. Non-equilibrium solidification of undercooled metallic melts [J]. *Materials Science and Engineering Reports*, 1994, 12: 177–272.
- [9] YANG Chang-lin, YANG Geng-cang, LU Yi-ping, CHEN Yu-zeng, ZHOU Yao-he. Phase selection in highly undercooled Fe–B eutectic alloy melts [J]. *Transactions of Nonferrous Metals Society of China*, 2006, 16(1): 39–43.
- [10] YANG Chang-lin, YANG Geng-cang, LIU Feng, ZHOU Yao-he. Purification and hypercooling of Fe–B eutectic alloy [J]. *Acta Metallurgica Sinica*, 2008, 44: 956–960.
- [11] WANG Hai-feng, LIU Feng, YANG Gen-cang, ZHOU Yao-he. Modeling the overall solidification kinetics for undercooled single-phase solid-solution alloys. I. Model derivation [J]. *Acta Materialia*, 2010, 58: 5402–5410.
- [12] WANG Hai-feng, LIU Feng, YANG Gen-cang, ZHOU Yao-he. Modeling the overall solidification kinetics for undercooled single-phase solid-solution alloys. II. Model application [J]. *Acta Materialia*, 2010, 58: 5411–5419.
- [13] GALENKO P K, DANILOV D A. Local nonequilibrium effect on rapid dendritic growth in a binary alloy melt [J]. *Physical Letters A*, 1997, 235: 271–280.
- [14] GALENKO P K, DANILOV D A. Model for free dendritic alloy growth under interfacial and bulk phase nonequilibrium conditions [J]. *Journal of Crystal Growth*, 1999, 197: 992–1002.
- [15] WANG Hai-fang, LIU Feng, CHEN Zheng, YANG Gen-cang, ZHOU Yao-he. Analysis of non-equilibrium dendrite growth in a bulk undercooled alloy melt: Model and application [J]. *Acta Materialia*, 2007, 55: 497–506.
- [16] WANG Hai-fang, LIU Feng, CHEN Zheng, YANG Gen-cang, ZHOU Yao-he. Effect of non-linear liquidus and solidus in undercooled dendrite growth: A comparative study in Ni–0.7 at.% B and Ni–1 at.% Zr systems [J]. *Scripta Materialia*, 2007, 57: 413–416.
- [17] KARMA A. Model of grain refinement in solidification of undercooled melts [J]. *International Journal of Non-equilibrium Processing*, 1998, 11: 201–233.
- [18] SCHWARZ M, KARMA A, ECKLER K, HERLACH D M. Physical mechanism of grain refinement in solidification of undercooled melts [J]. *Physical Review Letters*, 1994, 73: 1380–1383.
- [19] WANG Hai-feng, LIU Feng, TAN Yi-ming. Modeling grain refinement for undercooled single-phase solid-solution alloys [J]. *Acta Materialia*, 2011, 59: 4787–4797.

反向扩散效应对过冷单相固溶体合金凝固动力学的影响

王海丰, 刘峰, 王慷, 翟海民

西北工业大学 凝固技术国家重点实验室, 西安 710072

摘要: 基于平均体积方法建立过冷单相固溶体合金的凝固动力学模型并研究反向扩散在凝固动力学过程中的作用。模型在过冷 Ni–15%Cu(摩尔分数)合金快速凝固中的应用表明: 反向扩散显著影响凝固结束温度但对再辉阶段凝固的固相体积分数影响不明显。与 Herlach 观点相反, 凝固结束温度介于杠杆定律和 Scheil 方程的预测值之间, 且其具体值由反向扩散、初始过冷度和冷却速率决定。

关键词: Ni–Cu 合金; 快速凝固; 扩散; 过冷

(Edited by LI Xiang-qun)